

## Raman characterization of the optical phonons in $\text{Al}_x\text{Ga}_{1-x}\text{N}$ layers grown by MBE and MOCVD

A. Cros

Walter Schottky Institut, Technische Universität München  
and  
Dep. Física Aplicada, Univ. Valencia

H. Angerer, R. Handschuh, O. Ambacher, M. Stutzmann  
Walter Schottky Institut, Technische Universität München

This article was received on June 11, 1997 and accepted on October 8, 1997.

### Abstract

We present the results of Raman measurements performed on  $\text{Al}_x\text{Ga}_{1-x}\text{N}$  layers grown by MBE and MOCVD. The films were deposited on (0001) c-sapphire substrates, and the aluminum content covered the whole composition range for  $x$  from 0 (GaN) to 1 (AlN). It is shown that the energies of both  $A_1(\text{TO})$  and  $A_1(\text{LO})$  phonon modes smoothly increase with increasing  $x$ , indicating a one-mode behavior. The  $E_2$  phonon mode, however, presents a different behavior. Its energy increases very slowly with aluminum content and, for  $x \approx 0.4$ , a new phonon mode shows up which is shifted to higher energies by  $50 \text{ cm}^{-1}$ . This new line leads to the  $E_2$  AlN mode for increasing aluminum content. The linewidths and intensities of these modes strongly depend on composition. These results are compared with recent theoretical calculations. Finally, the Raman selection rules in the MBE and MOCVD samples are compared and conclusions about the quality of the layers are drawn.

### 1. Introduction

Many scientific groups have been attracted by the properties of the wide band-gap III-V nitrides in the last years. The progress achieved in the control of the growth and doping of GaN, AlN and their alloys, [1] and the successful application of these materials in the fabrication of optoelectronic devices, encourages increasing work on the characterization of the fundamental properties of these materials. The knowledge of these properties is important to determine the limits of their performance in device applications. Despite the successful fabrication of  $\text{GaN}/\text{Al}_x\text{Ga}_{1-x}\text{N}$  heterostructures showing two-dimensional electronic properties [2] and room-temperature stimulated emission, [3] the basic properties of  $\text{Al}_x\text{Ga}_{1-x}\text{N}$  are, to a large extent, unknown. [4] [5]

In this work, we study the Raman scattering spectra of  $\text{Al}_x\text{Ga}_{1-x}\text{N}$  alloys grown by plasma-enhanced molecular beam epitaxy (MBE) and metalorganic chemical vapor phase deposition (MOCVD). The optical phonons have been studied as a function of the aluminum content  $x$  for the whole compositional range ( $0 \leq x \leq 1$ ) for the MBE samples and for  $0 \leq x \leq 0.5$  for the samples grown by MOCVD.

Binary mixed crystals are classified into two main classes (one-mode and two-mode) according to the behavior of their optical phonons at the  $\Gamma$  point [6]. In the one-mode class, the frequencies of the different optic modes vary continuously and approximately linearly when changing the concentration of the alloy. On the other hand, in the two-mode type behavior two sets of optic modes are observed, each set corresponding to one of the two pure crystals which compose the alloy. These "extra" modes may persist very close to the end compositions ( $x \approx 0$  and  $x \approx 1$ ). The modes occurring in the composition region where the materials are almost pure have been attributed to either a local or a gap mode arising from a residual concentration of the minority component.

An investigation of the Raman spectra of  $\text{Al}_x\text{Ga}_{1-x}\text{N}$  films in the compositional range  $0 \leq x \leq 0.15$  has been already performed. [7] The authors analyzed the behavior of different phonon modes and could not find any evidence of a localized mode, finding a continuous change of the energy of the modes as a function of aluminum concentration. Consequently, they concluded that  $\text{Al}_x\text{Ga}_{1-x}\text{N}$  presents a one mode behavior. We have extended these studies to the whole compositional range of the alloy, analysing samples grown by two different methods (MBE and MOCVD). The experimental results are discussed in the light of recent theoretical calculations [8] and conclusions about the quality of the samples are made.

## 2. Experiment

Substrates of (0001) sapphire were chosen to grow epitaxial  $\text{Al}_x\text{Ga}_{1-x}\text{N}$  films by MBE and MOCVD to a layer thickness between 0.5 and 1  $\mu\text{m}$ . The substrate temperature was maintained between 800 and 850°C during MBE growth. For the samples grown by MOCVD, the growth chamber was kept at a pressure of 100 mbar, and the substrate temperature was 950°C. Before the deposition of the GaN film, a thin buffer layer ( $\approx 50$  nm) was grown at 550°C. For the MBE samples, however, no buffer layer was grown. The alloy composition was determined by elastic recoil detection analysis [9] (ERDA) and X-ray diffraction, with an absolute error smaller than 5%.

The Raman spectra were taken at room temperature in backscattering configuration from the (0001) surface of the wurtzite structure (z direction), and perpendicular to this surface (x direction). The Porto notation will be used to indicate the polarization configuration in which each spectrum was taken. The beam of an argon ion laser was used as exciting source (476.5, 488 and 515 nm). A microscope objective was employed to focus the laser on the sample surface to a spot size of about 2  $\mu\text{m}$ , with a power density of about  $10^5$  W/cm<sup>2</sup>. The Raman signal was analyzed with a triple spectrograph and detected with a cooled CCD camera. The lattice mismatch between film and substrate induces stress in the samples, which reflects in a shift of the phonon modes in the Raman spectra. This stress has been investigated by means of X-ray diffraction, and the corresponding Raman shift has been estimated to reach a maximum value of 3 cm<sup>-1</sup>. [10]

## 3. Discussion

To study the Raman selection rules, which allow the assignment of the phonon modes, we have plotted in Figure 1 the Raman spectra of an  $\text{Al}_x\text{Ga}_{1-x}\text{N}$  sample with 50% aluminum, measured in four different polarization configurations. This sample was grown by MBE under the same conditions as the other samples measured in this work. The only difference is that its thickness is somewhat greater (3  $\mu\text{m}$ ), to facilitate the measurement in the  $\mathcal{E}(-, -)\bar{\mathcal{E}}$  polarization configurations and minimize the contribution of the sapphire substrate to the spectra. The scale of the different spectra has been changed to fit them in the same plot. In the first configuration measured,  $\mathcal{E}(x, x)\bar{\mathcal{E}}$ , both  $E_2$  and  $A_1(\text{LO})$  phonon modes are allowed. [11] [12] The  $A_1(\text{LO})$  mode disappears when we change to crossed polarization  $\mathcal{E}(x, y)\bar{\mathcal{E}}$ , as expected from the Raman selection rules for a material with wurtzite structure. In the  $\mathcal{E}(x, x)\bar{\mathcal{E}}$  polarization configuration, where the  $A_1(\text{TO})$  is allowed, the selection rules are also fulfilled. We cannot say the same from the spectrum taken in the  $\mathcal{E}(x, y)\bar{\mathcal{E}}$  configuration. Here, the  $E_1(\text{TO})$  mode should be allowed, but instead the  $A_1(\text{TO})$ ,  $E_2(\text{GaN})$  and  $E_2(\text{AlN})$  phonon modes are seen. A similar failure of the Raman selection rules has been observed in GaN samples (see for example the work of H. Siegle et al. [12]) The  $E_1(\text{TO})$  mode, which should appear between both  $E_2$  modes, is not seen due to the width and intensity of the forbidden phonon lines. This failure of the selection rules can be explained by taking into account the multiple reflections which occur inside the  $\text{Al}_x\text{Ga}_{1-x}\text{N}$  films when the spectrum is taken from the side of the sample, and the fact that the incident light was not exactly normal to the sample surface.

Figure 2 shows some of the Raman spectra obtained in the  $\mathcal{E}(x, -)\bar{\mathcal{E}}$  backscattering configuration. These spectra have been obtained from the MBE samples with an aluminum content ranging from 0 (GaN) to 1 (AlN). The position of the different phonon modes is indicated with red circles ( $E_2$ ), empty green triangles ( $A_1(\text{TO})$ ) and full blue triangles ( $A_1(\text{LO})$ ). Two of the peaks observed in the spectra correspond to the sapphire substrate. Their position is indicated with a dashed line. Although the spectra have been measured in backscattering from the c axis of the wurtzite structure, the forbidden  $A_1(\text{TO})$  mode is clearly seen in all the

samples measured. This feature is still not understood, but could be related to the stress built on the samples during the growth process, as it is absent in the thicker  $\text{Al}_{0.5}\text{Ga}_{0.5}\text{N}$  sample whose spectrum is shown in Figure 1.

As the aluminum content of the alloy is increased, the phonon modes shift to higher energy, but the  $E_2$  line changes its energy much more slowly than the  $A_1(\text{LO})$  and  $A_1(\text{TO})$  lines. An interesting feature arises for an alloy composition of 36% aluminum, where a new mode is observed as a broad peak centered at  $629\text{ cm}^{-1}$ . The intensity of this line increases with increasing aluminum content, and it shifts slowly to higher energy towards the position of the  $E_2$  line of  $\text{AlN}$ . The line is indicated by arrows in the different spectra of Figure 2a. At the same time, the intensity of the  $E_2(\text{GaN})$  mode decreases, and for an aluminum content greater than 89% the peak cannot be detected anymore. This behavior indicates the existence of one  $E_2$  mode characteristic of  $\text{GaN}$  and one characteristic of  $\text{AlN}$  for an intermediate alloy composition (two-mode behavior).

A better insight into the behavior of the different phonon modes can be obtained from Figure 3, which shows the position of the phonon modes as a function of aluminum content. The  $A_1(\text{LO})$  (blue triangles) shows a one-mode behavior, although its dependence on aluminum content is not linear. In the region of  $600\text{ cm}^{-1}$ , the two mode behavior of the  $E_2$  mode (red dots) can be clearly seen. As can be seen in Figure 3, both modes ( $E_2(\text{GaN})$  and  $E_2(\text{AlN})$ ) have been simultaneously measured for an alloy composition ranging from 35% to 66% aluminum. The behavior of the  $A_1(\text{TO})$  phonon mode (green triangles) is unfortunately not so clear. We have looked for an  $\text{AlN}$  local mode by measuring in the  $\langle \bar{1}, \bar{1}, 0 \rangle$  configuration, in which the  $E_2$  phonon mode is forbidden. However, the  $E_2$  mode was visible in this configuration, and hindered the detection of an  $\text{AlN}$  local mode related to the  $A_1(\text{TO})$  phonon mode. The two-mode behavior of  $\text{Al}_x\text{Ga}_{1-x}\text{N}$  has been recently predicted by Grille et al. [8] for the  $\text{TO}$  phonon mode of an alloy of the cubic polytype, while the  $\text{LO}$  phonon mode is expected to show one mode. The authors use a random-element isodisplacement model (REI), from which they conclude that the different behavior of the two modes is due to the strong ionicity of the bonds and the coupling of the  $\text{LO}$  modes to the long range electric field associated with the vibration.

In Figure 4 we compare the Raman spectra from the MBE (black line) and MOCVD (blue line) samples for two typical samples with 19% aluminum content. The width of the  $E_2$  phonon peaks of both samples are comparable ( $7$  vs.  $8.5\text{ cm}^{-1}$ , see also Figure 5). However, a striking difference between both spectra is the presence of the  $A_1(\text{TO})$  phonon mode in the MBE sample, which is absent for the MOCVD sample. This line should be forbidden in backscattering from the  $c$  axis of the wurtzite structure, as we already mentioned in the discussion of Figure 2. It must also be pointed out that the position of the  $E_2$  phonon mode is slightly different for both samples (the peak of the MBE sample shifts  $2\text{ cm}^{-1}$  to higher energy), although their aluminum content is almost the same. The difference in peak position and presumably also the failure of the selection rules in the  $\langle \bar{1}, \bar{1}, 0 \rangle$  for the MBE sample, are stress-induced, due to the lattice mismatch between the layer and the substrate. The stress is reduced in the MOCVD sample by the existence of the buffer layer. The electron-phonon interaction shows up in the lower intensity of the  $A_1(\text{LO})$  phonon mode in the spectrum of the MBE sample [13]. This is due to the fact that the electron concentration is one order of magnitude higher in the MBE than in the MOCVD sample ( $2 \times 10^{18}\text{ cm}^{-3}$  vs.  $3 \times 10^{17}\text{ cm}^{-3}$  as determined by Hall measurements). The high electron concentration is thought to be due to oxygen contamination of the samples during growth. The damping of the plasma-phonon coupled mode increases with increasing electron concentration, with a corresponding decrease of the intensity of the Raman peak. [14] [15]

The peak centered at  $730\text{ cm}^{-1}$  (arrows), which appears in the spectrum of the MOCVD sample, arises from the  $\text{GaN}$  buffer layer ( $A_1(\text{LO})$  phonon mode). This has been determined by measuring a sample with only the buffer layer, whose spectrum is shown at the bottom of Figure 4 (red line) for comparison with the spectrum of the MOCVD sample (blue line).

The widths of the  $E_2$  phonon modes are compared in Figure 5 for both types of samples, where the full width at half maximum (FWHM) is shown as a function of alloy composition. The linewidth of the  $\text{GaN}$   $E_2$  mode quickly increases with aluminum content, while the  $\text{AlN}$   $E_2$  mode becomes narrower. The decrease of the linewidth of the  $E_2(\text{AlN})$  mode is observed in the MBE as well as in the MOCVD samples, and it cannot be attributed to a change in the crystalline quality of the samples. This behavior seems therefore characteristic of the mode itself. In the inset of Figure 5 we have plotted the relative intensities of the Raman signals of the  $E$

$E_2(\text{GaN})$  and  $E_2(\text{AlN})$  phonon modes as a function of aluminum content. It can be seen that the strength of the  $E_2(\text{AlN})$  line increases with respect to the  $E_2(\text{GaN})$  as the aluminum content is increased from 30% to 70%, as expected in a two-mode type semiconductor. [16] The maximum observed for  $x=0.8$  in the linewidth of the  $E_2(\text{AlN})$  phonon mode correlates with the crystalline structure of the alloy as studied by X-ray diffraction, and is attributed to stress and a higher structural disorder. The linewidth of the  $E_2(\text{GaN})$  phonon mode is comparable for the MOCVD and MBE samples up to an aluminum concentration of 30%. For higher concentrations the phonon line of the MOCVD samples becomes much broader, indicating a deterioration of their crystalline quality.

## 4. Conclusions

We have characterized the behavior of the optical phonons in  $\text{Al}_x\text{Ga}_{1-x}\text{N}$  films by means of micro-Raman spectroscopy. Both one and two-mode behavior are simultaneously observed in this III-V alloy system for different phonon modes. While the  $A_1$  phonon modes seem to show a one-mode behavior, the  $E_2$  phonon modes exhibit a two-mode type behavior. From the extrapolation of the data shown in Figure 2, the frequency of the Al local mode in GaN is estimated to be  $616\text{ cm}^{-1}$ , while the Ga gap mode in AlN would vibrate at  $605\text{ cm}^{-1}$ . The Raman spectra of samples grown by MBE and MOCVD have been compared, discussing the selection rules for the phonon modes, and conclusions about the quality of the layers have been drawn.

## Acknowledgments

One of the authors (A.C.) would like to thank the Ministry of Education of Spain for financial support and the Walter Schottky Institut for its hospitality.

## References

- [1] H. Morkoc, S. Strite, G. B. Gao, M. E. Lin, B. Sverdlov, M. Burns, *J. Appl. Phys.* **76**, 1363-1398 (1994).
- [2] JM Redwing, MA Tischler, JS Flynn, S Elhamri, M Ahoujja, RS Newrock, WC Mitchel, *Appl. Phys. Lett.* **69**, 963-965 (1996).
- [3] T. J. Schmidt, X. H. Yang, W. Shan, J. J. Song, A. Salvador, W. Kim, O. Aktas, A. Botchkarev, H. Morkoc, *Appl. Phys. Lett.* **68**, 1820-1822 (1996).
- [4] M.R.H. Khan, Y. Koide, H. Itoh, N. Sawaki, I. Akasaki, *Sol. St. Comm.* **60**, 509 (1986).
- [5] S. Yoshida, S. Misawa, S. Gonda, *J. Appl. Phys.* **53**, 6844 (1982).
- [6] I. F. Chang, S. S. Mitra, *Adv. Phys.* **20**, 359 (1971).
- [7] K. Hayashi, K. Itoh, N. Sawaki, I. Akasaki, *Sol. St. Comm.* **77**, 115 (1991).
- [8] H. Grille, F. Bechstedt, *J. Raman Spectr.* **27**, 201 (1996).
- [9] G. Dollinger, S. Fausermann, P. Maier-Komor, *Nucl. Instr. Meth. Phys. Res. B* **64**, 422 (1992).
- [10] W Rieger, T Metzger, H Angerer, R Dimitrov, O Ambacher, M Stutzmann, *Appl. Phys. Lett.* **68**, 970 (1996).
- [11] C. A. Arguello, D. L. Rousseau, S. P. S. Porto, *Phys. Rev.* **181**, 1351 (1968).
- [12] H. Siegle, L. Eckey, A. Hoffmann, C. Thomsen, B. K. Meyer, D. Schikora, M. Hankeln, K. Lischka, *Sol. St. Comm.* **96**, 943-949 (1995).
- [13] F.A. Ponce, J.W. Steeds, C.D. Dyer, G.D. Pitt, *Appl. Phys. Lett.* **69**, 2650-2652 (1996).

[14] A. S. Barker, M. Ilegems, *Phys. Rev. B* **7**, 743 (1973).

[15] H. R. Kuo, M. S. Feng, J. D. Guo, M. C. Lee, *Jpn. J. Appl. Phys.* **34**, 5628 (1995).

[16] A. S. Barker, A. J. Sievers, *Rev. Mod. Phys.* **47**, S1 (1975).

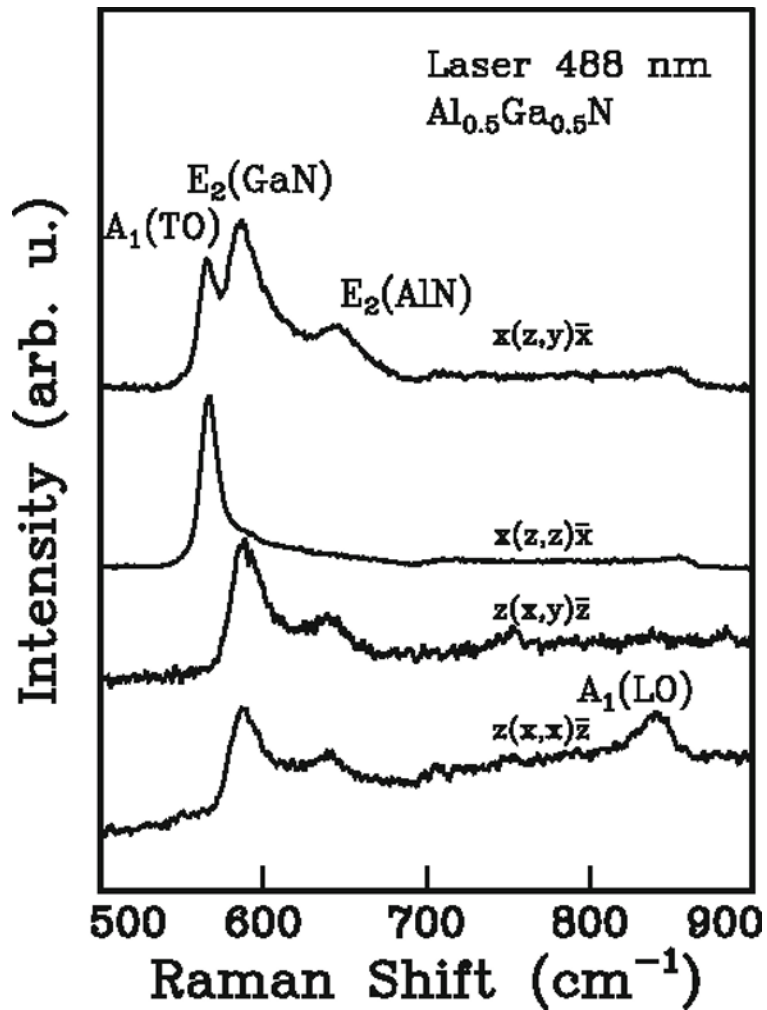


**Figure 1.** Room temperature Raman spectra of an  $\text{Al}_x\text{Ga}_{1-x}\text{N}$  sample with a thickness of  $3\mu\text{m}$  and an aluminum content of 50%. The polarization configuration used is indicated on each spectrum.

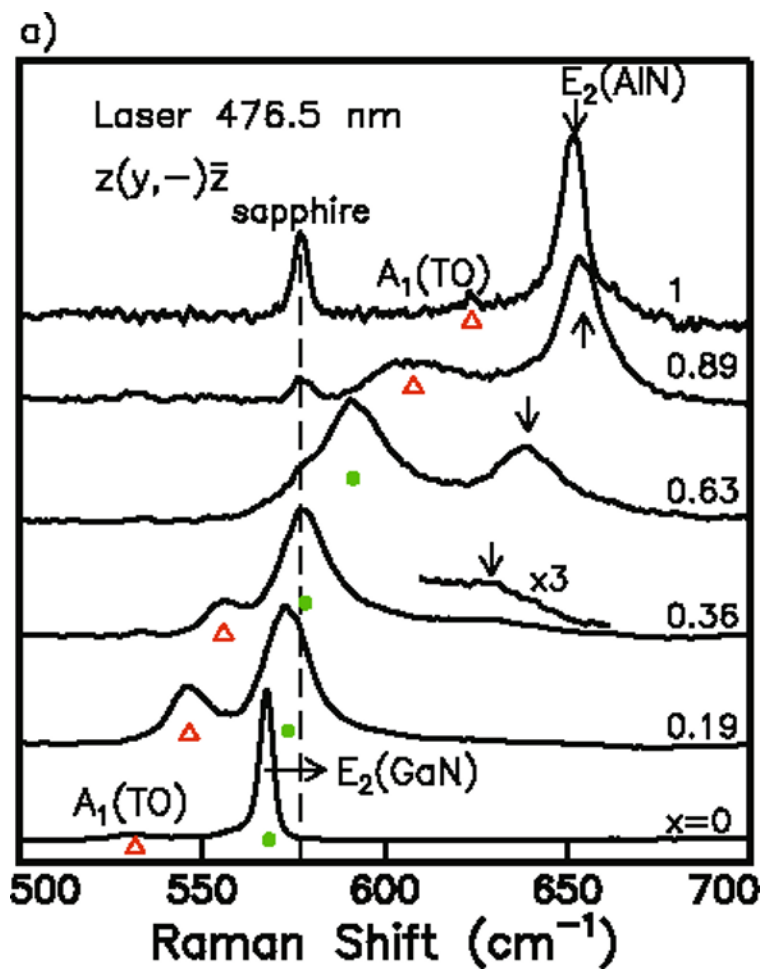


Figure 2a. Room temperature Raman spectra obtained for different  $\text{Al}_x\text{Ga}_{1-x}\text{N}$  compositions. Spectral range showing (a)  $A_1(\text{TO})$  (green triangles) and  $E_2$  (red dots and black arrows) phonon modes. The dashed line indicates the position of the modes related to the sapphire substrate.

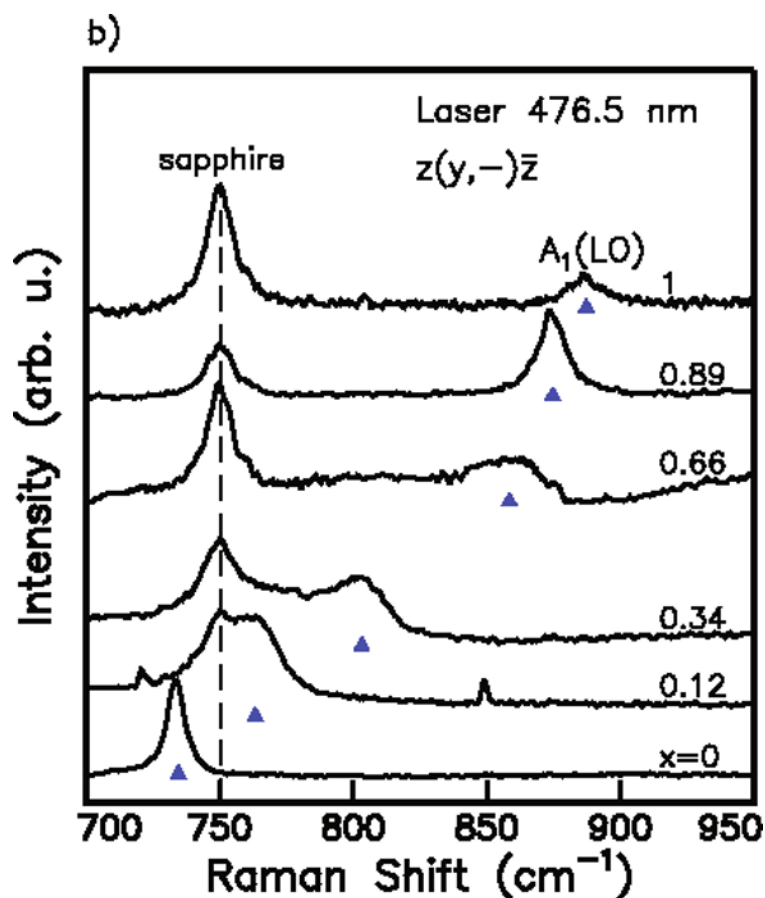


Figure 2b. Room temperature Raman spectra obtained for different  $\text{Al}_x\text{Ga}_{1-x}\text{N}$  compositions. Spectral range showing  $A_1(\text{LO})$  phonon mode (blue triangles). The dashed line indicates the position of the modes related to the sapphire substrate.



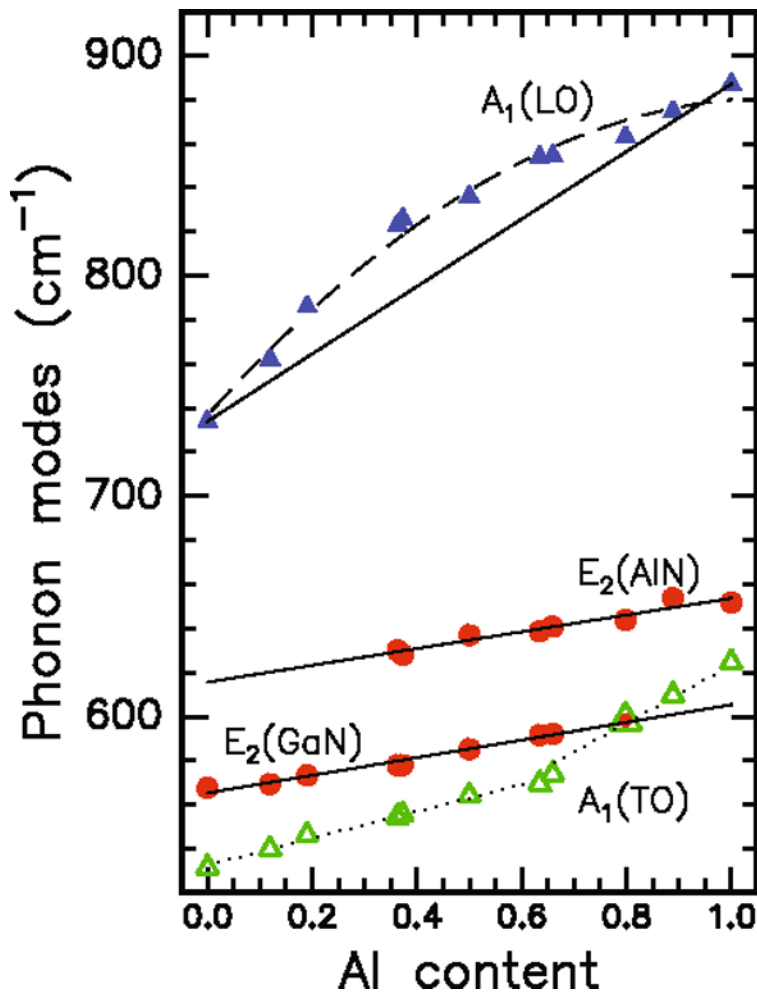


Figure 3. Dependence of the frequencies of the  $A_1(\text{TO})$  (green triangles),  $E_2$  (red dots) and  $A_1(\text{LO})$  (blue triangles) phonon modes on alloy composition.

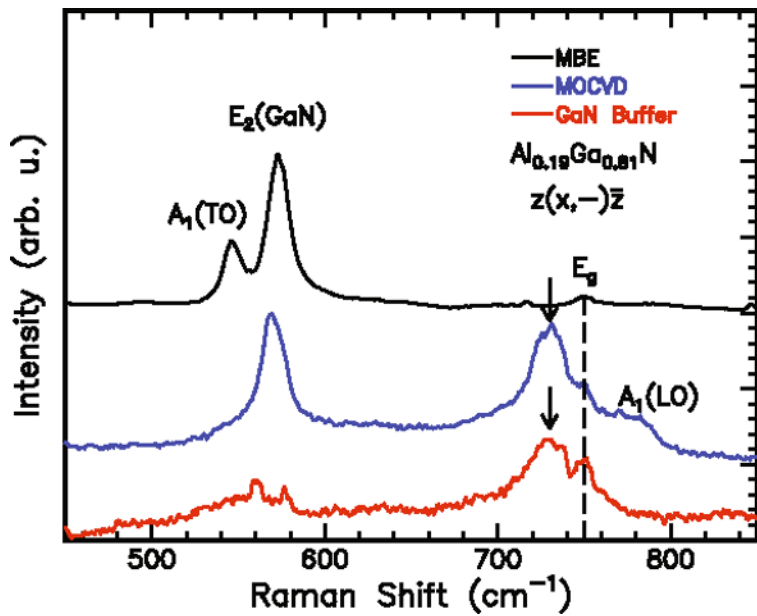
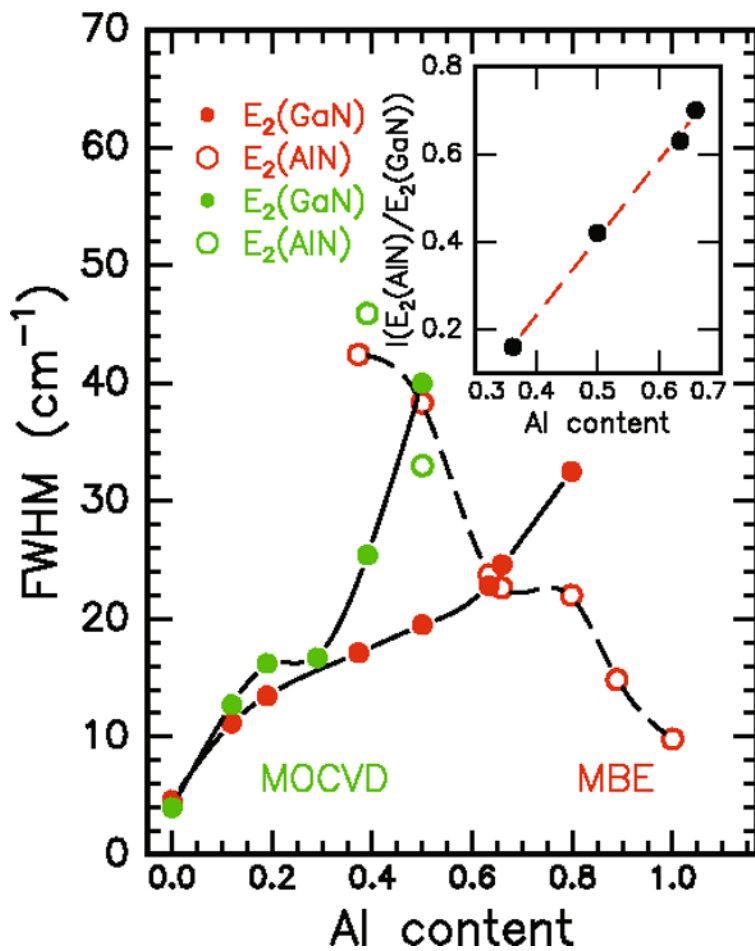


Figure 4. Room temperature Raman spectra of two  $\text{Al}_x\text{Ga}_{1-x}\text{N}$  samples grown by MBE (black) and MOCVD (blue) with an aluminum content of 19%. The spectrum of a sample with only a GaN buffer layer grown by MOCVD (red line) has been included for comparison with the spectrum plotted in blue. The dashed line indicates the position of the sapphire  $E_g$  mode. The arrows indicate the  $A_1(\text{LO})$  phonon mode arising from the GaN buffer layer.



**Figure 5.** Dependence of the linewidths of the  $E_2(\text{GaN})$  (full dots) and  $E_2(\text{AlN})$  (empty dots) phonon modes on aluminum content for the MBE (red) and MOCVD (green) samples. The lines are drawn as guides to the eyes. The inset shows the relative intensities of the  $E_2(\text{GaN})$  and  $E_2(\text{AlN})$  phonon modes as a function of aluminum content

© 1997 The Materials Research Society